• Lag bolt (for use on wood-frame buildings), and
• Masonry "PK" nails (for use on bituminous pavement or joints in concrete sidewalks or streets).

Surveying Equipment

Instrument: Lietz automatic level, Model Bl, with a polarizing lens. Rod: Use same rod for all readings. Invar rod should be used and preferably purchased for exclusive use on the project. A Wild Model GPCE 10 was used on this project.

Field Procedures

Field procedures included

• Maximum line-of-sight of 100 ft;
• Balanced backsights and foresights;
• Careful plumbing of rod;
• To the greatest extent possible, use of identical party members for all surveys;
• Identical level circuit to be used for all surveys;
• Use of good quality pavement turning points (i.e., such as PK nails or equivalent); and
• Rod readings to 0.001 ft.

Instrumentation for Load Transfer in Socketed Pier Foundations

R. G. HORVATH

ABSTRACT

An investigation of methods to improve the performance of drilled pier foundations socketed into soft rock was made on full-scale test piers. Instrumentation of the test piers enabled load transfer behavior of the piers to be studied. Flatjack (FREYSSI) load cells were used to measure applied loads and the end-bearing component of pier load support. Vibrating wire concrete embedment strain gauges (Geonor) were used to determine axial and radial stresses at the middepth of the test section. Thus, load distribution along the length of the pier socket could be determined. The description, calibration, and installation of the instruments are briefly summarized. The satisfactory performance and reliability of the instruments are supported by the test data that, in general, were in good agreement with predictions from elastic solutions. Comparison of the results of several piers having different support conditions, and displacement measurements using telltale systems, also support the reliability of these instruments. The versatility of a flatjack load cell to perform three different functions: (a) passive load cell, (b) active (applied) load cell, and (c) void, at the base of one test pier subjected to multiple loading cycles, is also briefly discussed.

Field load testing of six full-scale, instrumented concrete piers socketed into weak rock was carried out to investigate methods of improving the performance of this type of foundation system (1,2). A summary of the load testing program is given in Table 1.

To gain a better understanding of the load transfer mechanisms operating in socketed pier foundations, measurements were made of

• The portions of load supported by shift resistance and end bearing,
• Displacements at the top, middepth, and bottom of the socket,
• Displacements in the rock adjacent to the pier socket, and
• Strains within the concrete pier at middepth.

Presented in the following sections are a brief summary of the test conditions and a description and discussion of each instrument, which includes calibration, installation, performance, and reliability.

TEST CONDITIONS

To minimize construction costs and to simplify inspection, instrumentation installation, and construction, a shale quarry was selected as the test site because the work could be carried out directly

TABLE 1 Summary of Field Load Testing Program

	PIER DESCRIPTION		TEST DESCRIPTION
P1	Smooth Shaft Conventional construction Void at base		Shaft resistance only
P2	Smooth shaft Conventional construction Load Cell at Base		Shaft resistance and End-bearing resistance
P3	Roughened shaft Shaft grooved (AFE) Void at base		Shaft resistance only
P4	Roughened shaft Shaft grooved (AFE) Load cell at base		Shaft resistance and End-bearing resistance
P5	Smooth shaft Conventional construction Preload cell at base		Preload applied to base Shaft resistance and End-bearing resistance
		A	Preload = 0.89 MN
		B	Preload = 1.78 MN
		C	Preload = 4.00 MN
		D	Shaft resistance only
P6	Roughened shaft Shaft grooved (ART) Void at base		Shaft resistance only

Notes: All test piers were auger excavated and had the following dimensions:
Socket diameter, D_s = 710 mm
Socket length, L_s = 1370 mm
Aspect ratio, L_s/D_s = 1.9
All load tests were axial compression tests.

on the exposed rock surface. The site was located in Burlington, Ontario.

Material Properties

The rock exposed at the site consisted of predominantly weak red mudstone (Queenston shale) that became massive with depth. A summary of classification data and engineering properties of the shale is given in Table 2.

The average properties of the concrete were

Uniaxial compressive strength	σ_c = 49 MPa
Elastic modulus	E_s = 35 GPa
Poisson's ratio	v = 0.27

More detailed information concerning the material properties may be found elsewhere (1,2).

Test Pier Details

The dimensions of the test section of each pier were socket diameter D_s = 710 mm and socket length L_s = 1.37 m (Figure 1). The top of each test section was located approximately 0.6 m below the ground surface. The sockets for each test pier were excavated with a truck-mounted auger (Hughes-Williams LDH 100) that produced shafts with relatively smooth sides. Three test piers were constructed in shafts of this type. Three piers were constructed in shafts with grooves approximately 25 mm deep and 40 mm high cut into the wall to increase the roughness. Three of the test piers were constructed with voids between the bottom of the pier and the bottom of the socket to eliminate end bearing. The remaining three piers were constructed with load cells at their bases.

TABLE 2 Summary of Engineering Properties of Mudstone (Queenston shale)

Test Description			Test Results Range	Ave.
Unit Weight	γ	(kN/m^3)	25.8 to 26.1	25.9
Water Content	w	%	4.1 to 4.8	4.6
Liquid Limit	w_L	%	--	22
Plasticity Index	I_P	%	--	3
Rock Quality Designation	RQD	%	29 to 88	70
Shore Scleroscope Hardness	S_h		14 to 19	16
Point Load Strength	$I_s(50)$	(MPa)	0.56 to 0.91	0.69
Brazilian Tensile Strength	σ_t	(MPa)	0.21 to 1.03	0.64
Uniaxial Compression Test				
Compression strength	σ_c	(MPa)	4.70 to 11.10	6.75
Secant elastic modulus	E_s	(MPa)	400 to 1180	695
Poisson's ratio	v		0.19 to 0.35	0.30
Triaxial Compression Test (σ_3 = 0.7 to 3.5 MPa)				
Cohesion	c	(MPa)	--	1.2
Friction	ϕ	(deg)	--	43
Secant elastic modulus	E_s	(MPa)	500 to 1600	1000
Poisson's ratio	v		--	0.22
Direct Shear Test				
Peak:	c	(MPa)	--	0.3
(σ_n = 0.3 to 0.6 MPa)				
	ϕ	(deg)	--	54
Residual:	c	(MPa)	--	0
(σ_n = 0.3 to 2.8 MPa)				
	ϕ	(deg)	--	29
Goodman jack				
Elastic Modulus	E_g	(MPa)	740 to 1420	1085

Reactor Frame

The main components of the load-reaction system were the reaction beam, anchor piers, and the anchor connections (Figure 2). The system was designed for a maximum safe test load of 8.7 MN.

Instrumentation

Suitable monitoring equipment was selected to provide the basic data necessary to study the load transfer behavior of socketed piers. Profiles of the

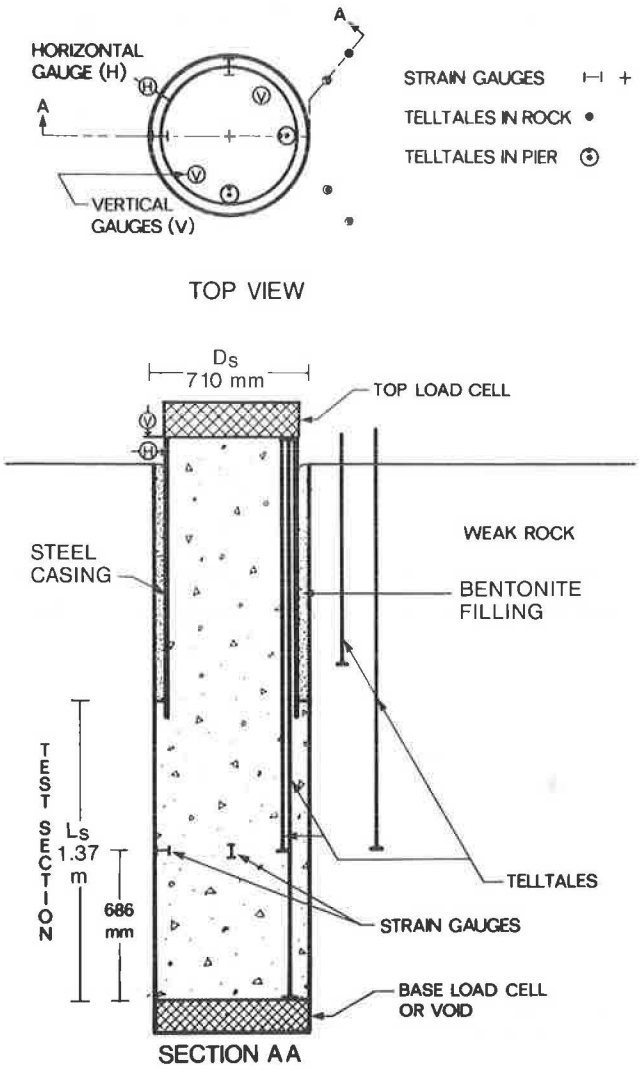

FIGURE 1 Typical test pier and instrumentation.

wall of each socket were made using a simple profilometer. The profilometer was basically a pantograph instrument, consisting of a feeler arm that followed the surface of the rock and a tracing arm that recorded the profile on paper.

Measurements of vertical displacements were made at two locations on top of each pier with dial indicator gauges fastened to wooden reference beams supported outside the influence of the test (approximately 2.5 m from the pier). Within each pier and in the surrounding rock, vertical displacements were measured using telltale rods and dial indicator gauges (Figure 1).

The test loads were applied and measured by means of oil-filled FREYSSI flatjacks. This type of flatjack was also used to measure end-bearing loads. Vibrating wire strain gauges were installed within the test piers for the purpose of estimating axial and radial stresses in the concrete during loading.

Construction and Instrumentation Installation

Each test pier was constructed individually to ensure that the concrete was placed on the same day that the socket shaft was drilled. The test piers were constructed between April 3 and April 18, 1980, and tested between May 17 and June 18, 1980. The sequence of construction and instrument installation was generally the same for each test pier. The steps were

1. The shaft was drilled with the auger to the required depth.
2. The shaft was visually logged, photographed, and tested with a Schmidt Hammer. Four profile traces, at 90-degree spacing, were made with the profilometer at the top and bottom of the test section.
3. Grooving of the socket wall (P3 and P4) was carried out at this point. Step 2 was repeated except for the Schmidt Hammer testing.
4. The bottom of the drilled socket was cleaned as required. Test piers P2, P4, and P5 were thoroughly cleaned by hand to provide a good clean surface for the bottom load cells.
5. A thin layer of grout was placed on the bottom of the socket (P2, P4, and P5 only) to provide a smooth contact surface for the load cells.
6. The load cell (P2, P4, and P5), or the void-forming device (P1, P3, and P6), was placed in position at the base of the socket.
7. Concrete was placed up to the middle of the test section and vibrated.
8. The concrete embedment strain gauges were installed (except P6).
9. The upper casing and telltale assemblies were placed in position.
10. Concrete was placed up to the top of the test section and vibrated.
11. After the concrete in the test section had set (next day) the casing above the test section was filled with concrete and vibrated.

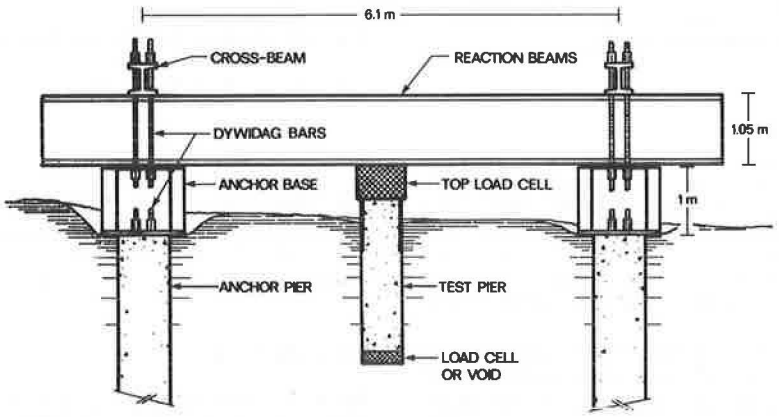

FIGURE 2 Load reaction frame system.

12. The annulus between the casing and the shaft, above the test section, was filled with bentonite to seal off any surface water.

13. Just before testing, the top of the pier was dry packed with grout to provide a smooth, level surface for installing the load transfer plates for the jacking system.

Load Application Procedure

A method of maintaining a constant rate of loading, similar to that used by Bozozuk et al. (3), was used for the tests. Load increments of 22 kN were applied at 15-min intervals. Each load was maintained for 13 min, and 2 min were allowed for adding the next load increment. Vertical displacement gauges at the top of the pier were read at 0-, 3-, 6-, 9-, and 13-min intervals for each load increment. Reading of all instruments, including horizontal displacement, rock displacement, strain gauges, and survey level, were taken at the 13-min mark.

Two test piers, P2 and P4, representing typical pier loading conditions (both shaft resistance and end-bearing resistance) were loaded in increments to 4.45 MN. This load was maintained for approximately 36 hr to observe possible changes of load-transfer behavior with the passage of time. On completion of the maintained-load portion of the test, incremental loading was resumed.

LOAD MEASUREMENTS

The loads applied to the top of the test piers and, in some tests, the loads transferred to the base of the socket in end bearing were both measured with load cells. The basic unit for each load cell was a FREYSSI flatjack pressure capsule that measures load hydraulically. All the load cells were calibrated before they were used in the field. The calibrations were obtained by duplicating in-service conditions as closely as possible.

Bourdon-type pressure gauges were used to measure the hydraulic pressure in the flatjacks. Two sets of gauges (0 to 6.9 MPa and 0 to 34.5 MPa) were used. The low-capacity pressure gauges were used to improve the accuracy at the lower stress levels. The gauges selected were accurate within ±1.5 percent.

Top Load Cell

The top load cell is unusual in that flatjacks were used for both applying and measuring the test loads. This load cell consisted of three to six 920-mm-diameter flatjacks positioned in series (Figure 3). The rated capacity of the flatjacks at a working hydraulic pressure of 14 MPa was 8.68 MN. Each flatjack was capable of expanding to a maximum opening of 25 mm.

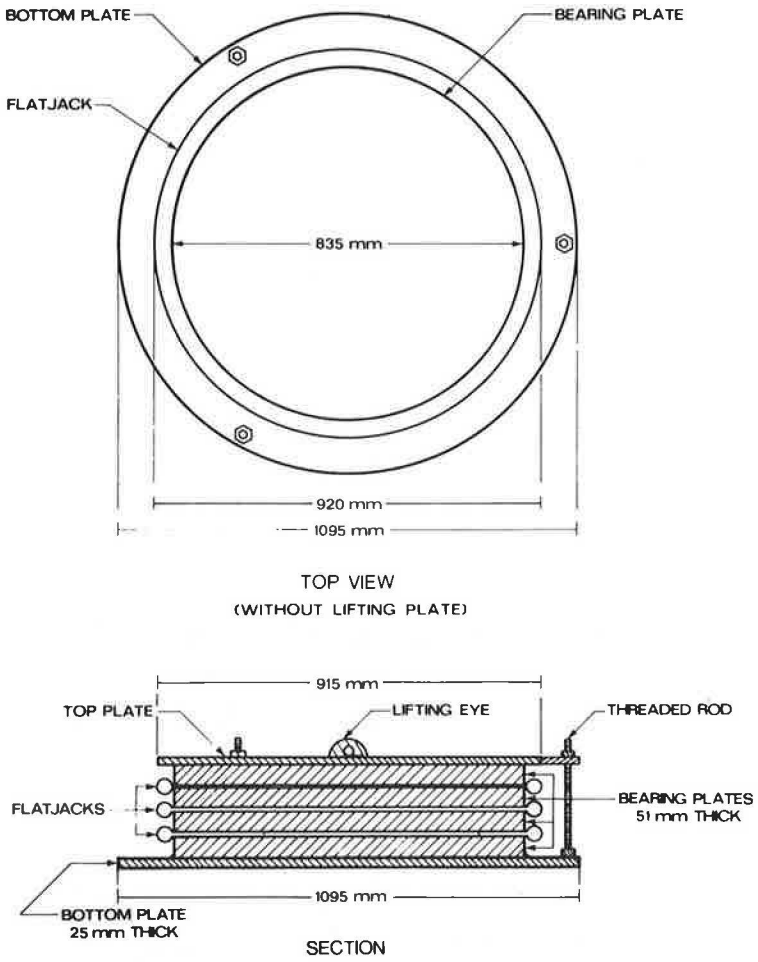

FIGURE 3 Top load cell.

Initially two of the flatjacks (partially expanded) were used as passive load cells. The remaining jacks were used as active jacks; that is, they were expanded by pumping hydraulic fluid into the jack thus applying the desired load to the top of the test pier. However, due to problems related to the lateral stability of the flatjack system, it was necessary to modify the procedure. Subsequently, all jacks in the system were initially deflated. A single flatjack was then inflated to near its maximum aperture (25 mm), closed off using the appropriate valves, and maintained as a passive load cell. If additional vertical movement was necessary, another flatjack was activated and the procedure was repeated.

The advantages of using flatjacks for applying the test load include

- At high loads, there is no problem with ram friction that can occur with piston-type hydraulic jacks;
- As long as the top surface of the pier is perpendicular to the shaft, the applied load will be parallel to the pier axis; and
- It is relatively easy to ensure that the applied load is concentric.

The top load cell performed well throughout the testing program. However, two incidents of equipment failure occurred that must be mentioned because they concern safety. It is important to note that both mishaps could have been avoided.

In the first case, a section of steel pressure tubing connected to one of the flatjacks pulled out of its fitting at a load of about 8 MN. Consequently a high-velocity stream of hydraulic fluid was expelled from the flatjack and covered a car about 10 m away. After this accident, all hydraulic fittings were changed to threaded-type connections. A partial shield (sheetmetal) was also installed around the top load cell to protect personnel.

In the second case, one flatjack ruptured at a load of about 7.5 MN. The high-velocity stream of oil expelled from the flatjack bent the protective shield and traveled about 10 m. The rupture occurred because the test pier had been accidentally constructed approximately 150 mm off the centerline of the load reaction frame. Consequently, the reaction frame and load cell were subjected to severe lateral and twisting distortion during loading.

Base Load Cells

The base load cells were made up of two or three 600-mm-diameter flatjacks positioned in series (Figures 4 and 5). The rated load capacity of these flatjacks was 3.46 MN at a working pressure of 14 MPa. The maximum displacement capacity was 25 mm for each flatjack. Two flatjacks were expanded approxi-

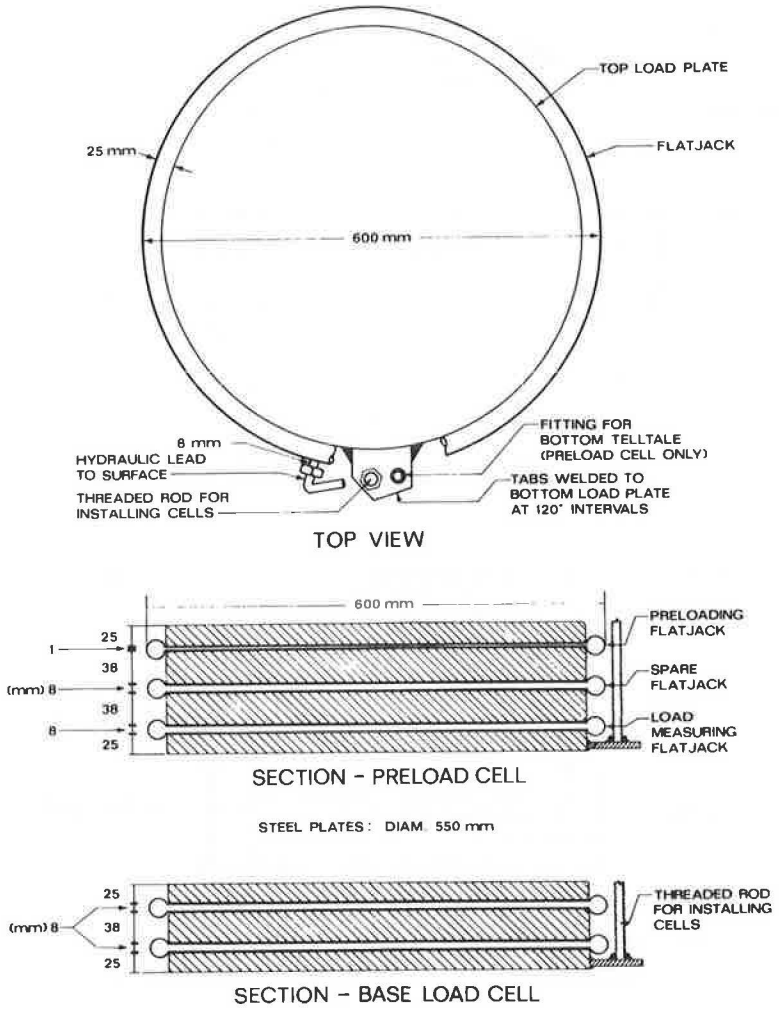

FIGURE 4 Base load cells.

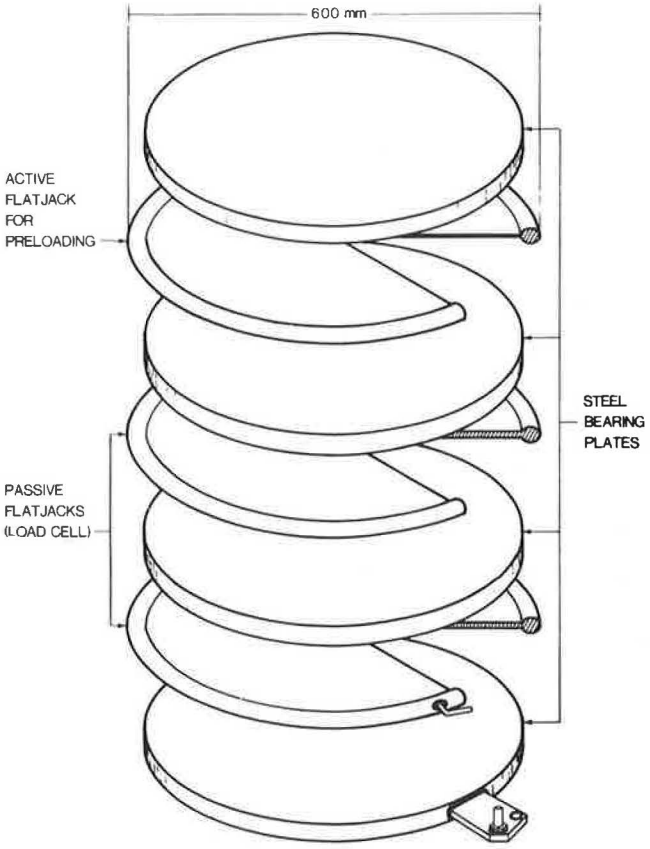

FIGURE 5 Base load cell—exploded view.

mately 6 mm before being placed at the base of the excavation. These cells were connected to pressure gauges in a closed hydraulic system and were used to monitor the load transferred to the bottom of the test piers. Only one flatjack was necessary for this purpose. However, a second one was included as insurance in case there was a malfunction of the first one.

A multiple-loading test procedure was developed to observe the effects of preloading the base of a drill pier in weak rock to improve the load-displacement performance (1). To implement the multiple-loading method, a suitable preload cell was required at the bottom of the test pier. This preload cell was capable of performing three different functions: (a) measuring the load transferred to the end bearing at the pier base (passive load cell), (b) applying a load at the pier base (active load cell), and (c) eliminating end-bearing load (void). The preload cell used for the cycled loading test on this project (1) consisted of three oil-filled FREYSSI flatjacks positioned in series (Figures 4 and 5). All three flatjacks were partly expanded to about 6 mm and calibrated before being placed in the test pier shaft.

A brief explanation of the versatility of the preload cell may be provided by a description of how the cell could function during different loading cycles. During loading cycle A (combined shaft resistance and end-bearing resistance), all three flatjacks could be used as passive load cells. Each flatjack would be connected to a pressure gauge (or transducer) in a closed hydraulic system to monitor the load transferred to end bearing at the bottom of the pier. For loading cycle B (end-bearing resistance only), one flatjack, an active load cell, would be connected to a hydraulic pump. This flatjack could then be expanded by pumping oil into it so that a load would be applied to the pier base. The other two flatjacks would continue to function as passive load cells. Loading cycle C (shaft resistance only) would be carried out with the valves for all three flatjacks opened. Thus, there would be no resistance to compression of the flatjacks back to their original shape. End-bearing resistance would therefore be essentially eliminated. Details of a recommended method for field testing drilled piers using a multiple-loading method are presented elsewhere (4).

Including a spare flatjack in the load cells proved to be a worthwhile precaution because one of the flatjacks in the preload cell began to leak during the initial portion of a test. The faulty flatjack was isolated from the system by opening the valve to the atmosphere, while pumping oil into the other two flatjacks until the faulty flatjack was completely compressed. The load test was then restarted using the two remaining flatjacks in the base load cell.

Calibration

The flatjacks for the top load, base load, and preload cells were calibrated using the 5.3-MN Baldwin Testing Machine at the University of Toronto. The calibration of the top load cell (8.25-MN capacity) was also verified on the 17.8-MN capacity testing machine at the Department of Mines and Resources, Elliot Lake Laboratory for Mining Research, Canadian Centre for Mineral and Energy Technology.

Representative calibration curves for the various load cells are shown in Figures 6-8. The gauge pressure-versus-load calibration curves for flatjack 6 of the top load cell and the top flatjack of the base load cell (cell 2) are shown on Figures 6 and 7, respectively. These curves were determined using linear regression analyses. The curve for flatjack 6 of the top load cell (Figure 6) is based on 190 data points (10 loading and unloading cycles) and had a coefficient of correlation, $r^2 = 0.9997$. The curve for the top flatjack of base load cell 2 (Figure 7) is based on 144 data points (8 loading and unloading cycles) having $r^2 = 1.0000$.

The load-versus-displacement calibration curve for base load cell 2 is shown in Figure 8. This curve was determined using the continuous plotting device on the testing machine. Eight cycles of loading and unloading were used and the curve of best fit (straight line) for each cycle was almost identical. The maximum deviation of any data "point" from the average curve was about 6 percent.

Reliability

The flatjack load cells performed well and, on the basis of the calibration testing and load testing results, the loads measured during the field testing were presumed to be accurate to about ±2 percent.

An indirect evaluation of the reliability of the base load cell measurements may be made by comparing the load-displacement curves for two test piers, P1 and P2, that were both constructed using conventional auger techniques. P1 had a void at its base (shaft resistance only) and P2 had a load cell at its base (combined shaft and end-bearing resistance). A comparison of the shaft resistance-versus-displacement curves for the two piers indicates almost identical behavior in terms of shaft resistance (Figure 9). Shaft resistance for P1 was measured

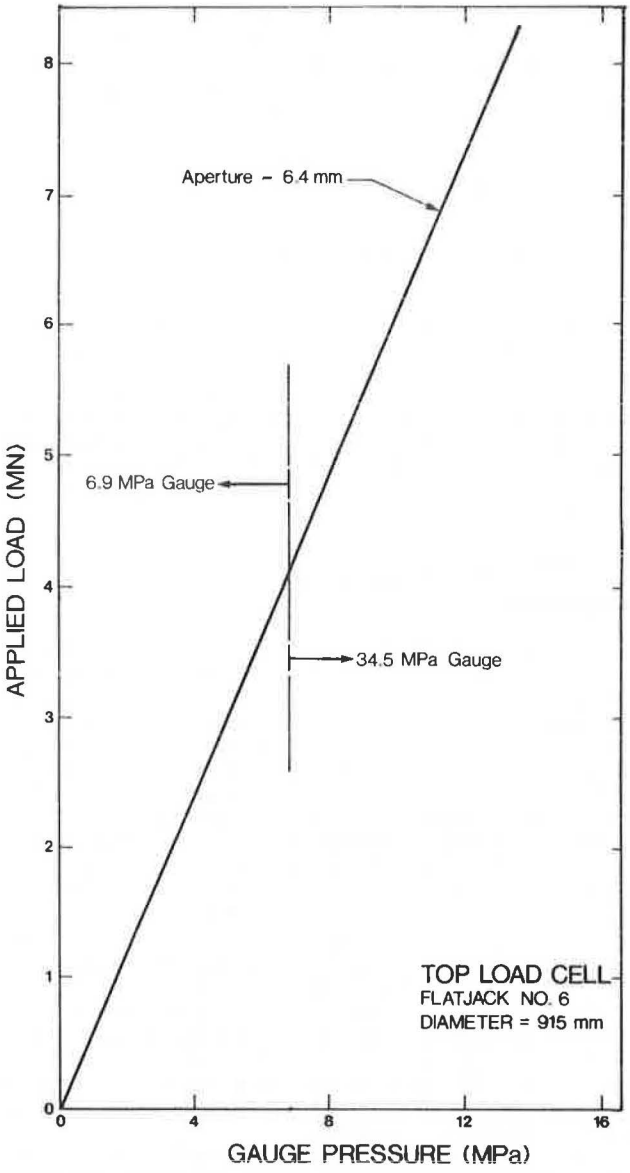

FIGURE 6 Calibration curve, applied load cell, flatjack 6.

directly, whereas shaft resistance for P2 was calculated using

$$Q_s = Q_t - Q_b \quad (1)$$

where

Q_s = shaft resistance load,
Q_t = applied load, and
Q_b = end-bearing load (measured using load cell).

This comparison suggests that the end-bearing loads measured by the base load cell are reliable. The reliability of the base load cells was also supported by a comparison of the results with behavior predicted on the basis of elastic analyses. A summary of a comparison of measured values of base load and predicted values using elastic solutions (5) is given in Table 3. The agreement between measured and predicted values is extremely good.

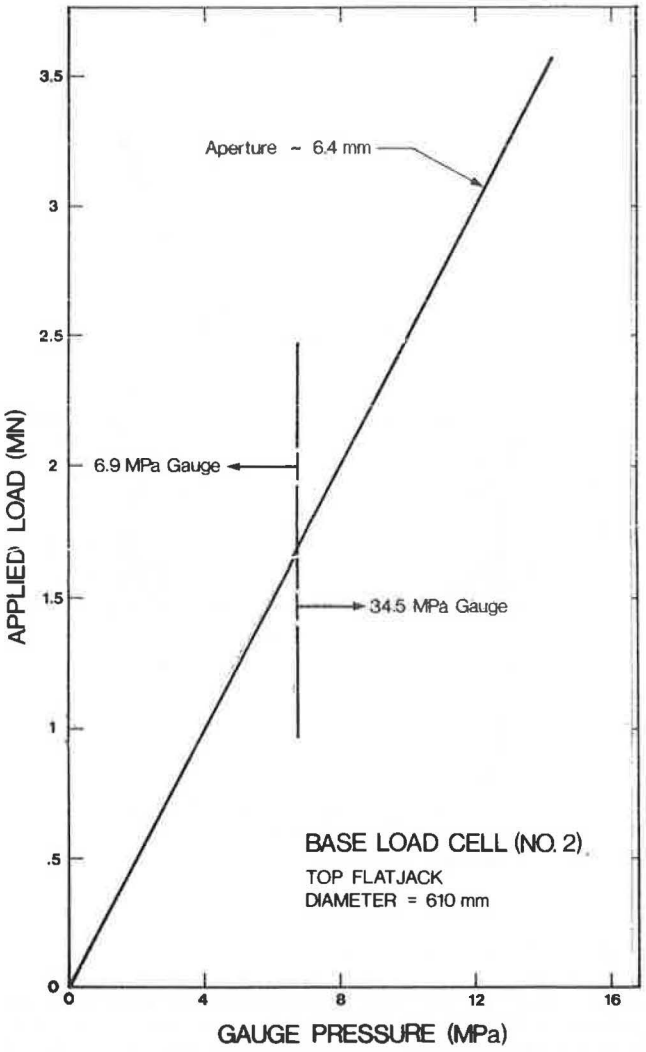

FIGURE 7 Calibration curves, base load cell 2, top flatjack.

Only one flatjack, out of the seven used for the base load cells, failed to operate. This failure was presumed to have been caused by a leak in a pressure-tubing connection, which may have been damaged during installation.

DISPLACEMENT MEASUREMENTS

Vertical and horizontal displacement measurements for the piers were made using dial indicator gauges (0.025 mm per division). The measurements were referenced to timber beams supported on steel rods driven into the soft rock. A survey level and steel scales (1-mm divisions) were used to cross check vertical displacement at the top of the test piers, to measure vertical uplift of the anchor piers, and to verify that the reference beam supports did not move.

Pier Displacements

Vertical displacements were measured at the top of the test pier at two locations 180 degrees apart (Figure 1), at middepth, and at the bottom of the test section at two locations each 90 degrees apart,

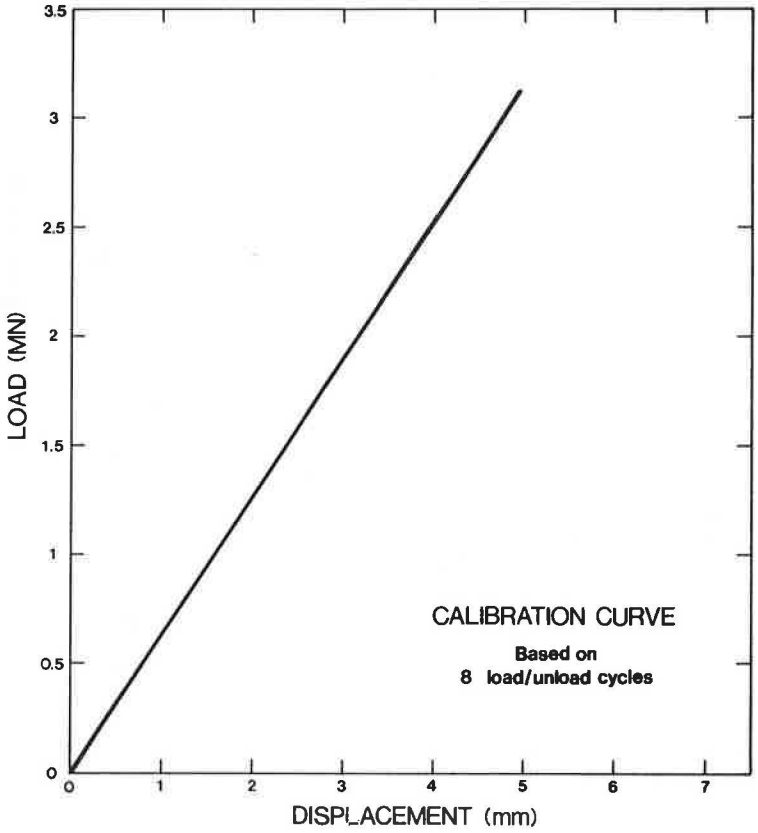

FIGURE 8 Calibration curves, base load cell 2—load versus displacement.

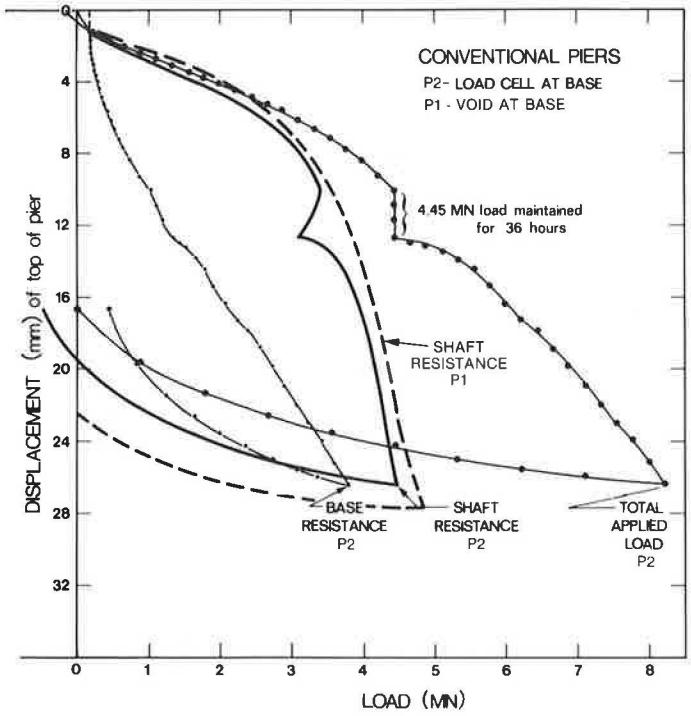

FIGURE 9 Comparison of load-displacement behavior for test piers P1 (shaft resistance only) and P2 (shaft resistance and end bearing).

TABLE 3 Comparison of Measured and Predicted Values of Base Load (Q_b/Q_t)

	TEST PIER		
	P2	P4	P5
Applied Load, Q_E (MN)	2.2	2.4	*2.1
Q_b/Q_t (measured)	.15	.20	*.20
Q_b/Q_t (predicted by elastic analyses)	.20	.20	*.20

* average value based on several test cycles

using a system of telltale rods (Figure 1). The telltale system consisted of a threaded rod inside a copper tube sleeve. A large washer was fastened to the base of the rod for embedment in the concrete. Tape was used as a spacer between the washer and the tubing to allow vertical movement of the rod and to seal the bottom of the tube to prevent concrete from seeping in. Dial gauges referenced to the top of the test pier were used to measure these telltale displacements. The telltale systems were only intended to measure displacements and did not provide the precision or accuracy necessary to determine strains within the pier. Typical load-displacement curves for a test pier are shown in Figure 10.

Horizontal displacement was measured at the top of the test pier at one location.

Rock Displacements

Vertical displacements within the rock mass adjacent to the test piers were measured at approximate depths of 0.9 m and 1.8 m at two locations using telltale rods (Figure 1). The telltale system consisted of threaded rods grouted at the bottom of a 50-mm-diameter percussion-drilled hole. The holes were located at distances of about 300 mm and 600 mm outside the pier-rock interface. Displacements were measured using dial gauges attached to the wooden reference beams. Typical load-displacement curves for the rock adjacent to the test pier are shown in Figure 11.

STRAIN MEASUREMENTS

Description

Geonor P-250 embedment vibrating wire strain gauges were installed in all of the test piers (except P6) at the midpoint of the test section.

Three gauges were used in each pier: a single gauge located on the axis and oriented to measure axial strain and two gauges (90 degrees apart) located near the perimeter and oriented to measure radial strain (Figure 1). The three gauges were fastened to a frame, made from copper tubing, and were placed in position after the concrete had been placed up to the midpoint of the test section.

The strain gauge measurements were used to estimate axial and radial stresses acting at the midpoint of the pier test sections during load testing so that load or stress distribution along the socket length could be determined. The axial and radial stresses may be calculated from strain measurements using the following linear elastic equations for an axisymmetric pier (6):

$$\sigma_z = \{[E_c(1 - v_c)]/[(1 - 2v_c)(1 + v_c)]\}\{\varepsilon_z + [v_c/(1 - v_c)]\varepsilon_r + [v_c/(1 - v_c)]\varepsilon_\theta\} \quad (2)$$

$$\sigma_r = \{[E_c(1 - v_c)]/[(1 - 2v_c)(1 + v_c)]\} \times \{[v_c/(1 - v_c)]\varepsilon_z + [v_c/(1 - v_c)]\varepsilon_\theta\} \quad (3)$$

where

E_c = Young's modulus of the concrete,
v_c = Poisson's ratio of the concrete,
ε_z = the axial strain (measured),
ε_r = the radial strain (measured), and
ε_θ = the circumferential strain ($\varepsilon_\theta = \varepsilon_r$ assumed).

The pier is assumed to be isotropic and elastic and to have a uniform distribution of radial and axial strain across the pier section.

It should be noted that the use of strain measurements to estimate stress in concrete is not an

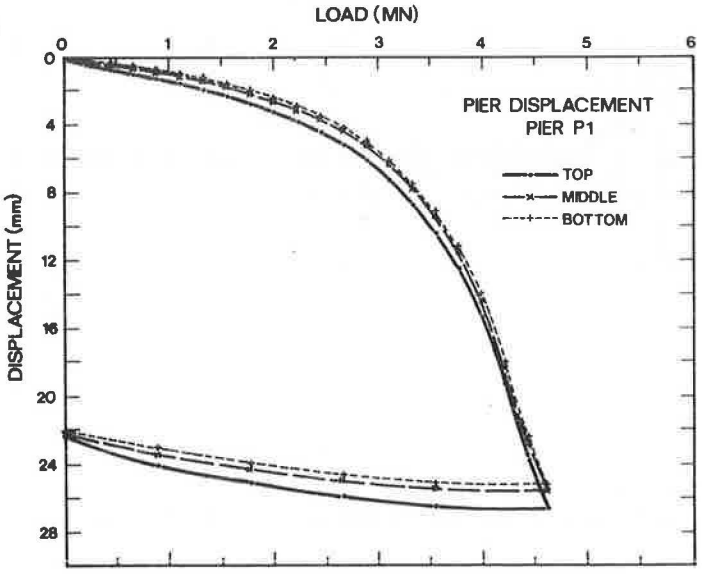

FIGURE 10 Typical load-displacement curves for test pier.

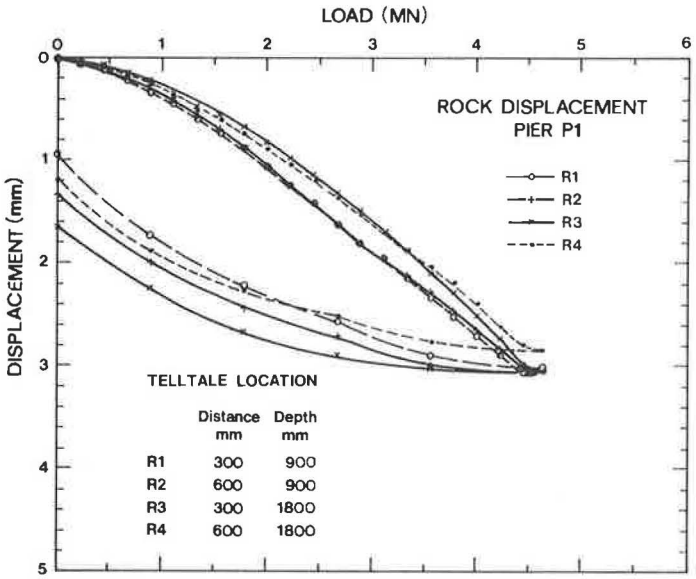

FIGURE 11 Typical load-displacement curves for rock adjacent to test piers.

ideal approach to the determination of load distribution. Knowledge of the elastic modulus of the concrete is necessary, and nonhomogeneity, stresses induced by curing, and creep behavior of the concrete can cause difficulties in the interpretation of the data.

The testing was of short duration; therefore, the influence of concrete creep on strain measurements would be negligible. Strain measurements were also obtained when the concrete was placed and at various intervals before testing (concrete curing period). All of the strain gauges indicated that concrete expansion occurred during curing.

Calibration

The strain-frequency calibration factor supplied by Geonor was verified in the laboratory. The reported accuracy of these gauges is ±2 microstrain over a range of 1250 microstrain.

Reliability

Some difficulties experienced with the electronics during load testing on piers P3 and P4 were traced to inadequate grounding of the readout instrument. After this problem was corrected, the strain measuring system functioned well. The reliability of the strain gauge measurements may be indirectly assessed by comparing the measured strains to expected values of strain for the various load support conditions.

Load tests were performed on conventional piers that had essentially zero base resistance. Thus, the applied load was supported only through shaft resistance. In these tests, the measured radial strains were negative (compression) indicating that the pier was being compressed radially inward during loading (Figure 12a). This behavior indicates the tendency for shear dilation (volume expansion) to occur at the pier-rock interface or within the rock, or both. Also, the strain data were consistent in that both axial and radial strains decreased (compression) with increasing applied load. Load tests were also carried out on piers with combined shaft resistance and base resistance components. In all of these tests, the measured radial strains were positive, indicating that the pier was expanding in a radial direction (Figure 12b). This behavior is comparable to that which occurs during a compression test on a concrete cylinder and indicates Poisson's effect. These strain data were consistent in that axial strain decreased (compression) and radial strain increased (expansion) with increasing applied load. Thus, all of the measured strain data correctly reflected the anticipated strain behavior for the load support conditions tested.

A summary of a comparison of values of axial strain measured using the strain gauges with values measured using the telltale systems and with values estimated using a simplified elastic analysis is given in Table 4.

The reliability of the data obtained from the vibrating wire strain gauges may also be assessed by examining the load distribution in the test piers. This is discussed in the next section. In the simplest case, test pier P1 (shaft resistance only), the determined load distribution was exactly as anticipated. Thus the strain gauge performance in this case can be judged to be extremely good. In the other test piers, the conditions were more complicated: combined end-bearing and shaft resistance, grooved shafts, preloading of base, and cycled loading were involved. Thus the reliability of the strain gauge measurements in these cases could not be evaluated.

LOAD DISTRIBUTION IN TEST PIERS

Load distribution in test piers P1 through P5 was determined from measurements of applied load at the top of each pier, axial and radial strain at the middepth of the test sections, and end-bearing load (or known boundary condition) at the base of each pier. Thus, the load distribution curves determined for all the piers were based on data from the same three locations. The top and bottom loads were measured with load cells except in the case of piers that had voids at their bases for which zero end-bearing load was assumed. The load (or stress) at pier middepth was determined indirectly using vibrating wire strain gauges embedded in the concrete pier.

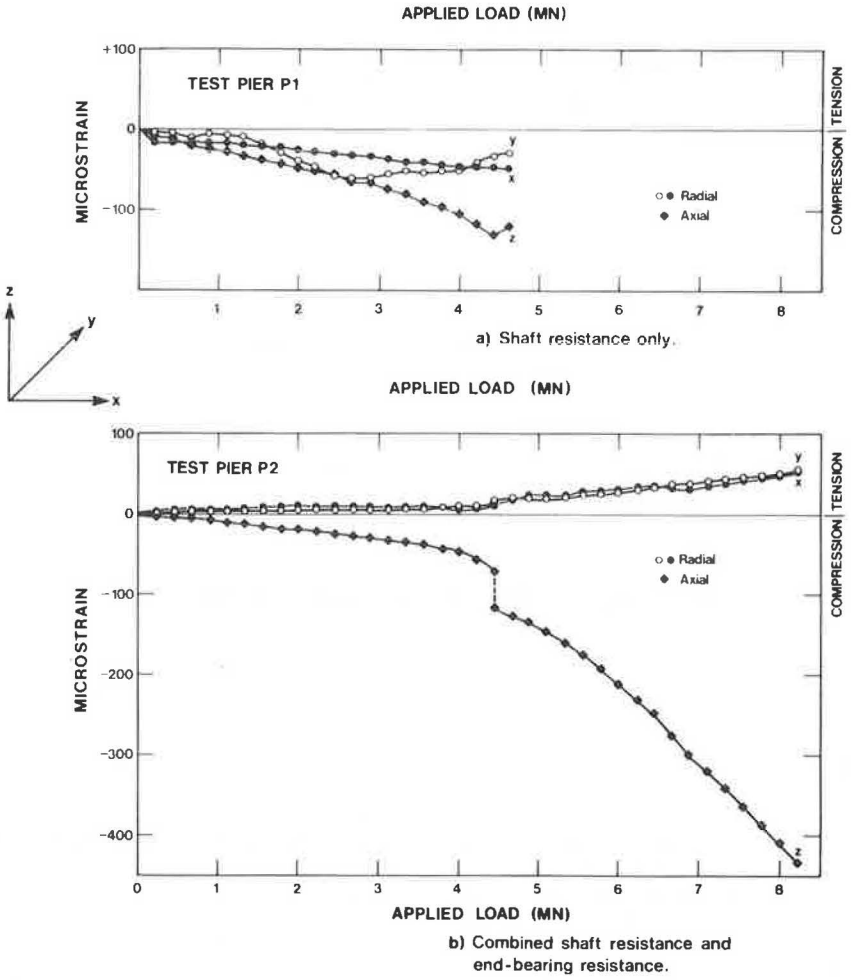

FIGURE 12 Measured values of axial and radial strain.

TABLE 4 Summary of Estimated and Measured Values of Axial Strain

		STRAIN IN PIER @ Q_a = 2 MN ($\times 10^{-6}$)			
		CALCULATED		MEASURED	
	PIER DESCRIPTION	Upper Limit	Best Estimate	Strain Gauge	Telltales*
P1	Conventional - void at base	41	21	46	110
P2	Conventional - end bearing	30	17	18	0
P3	Grooved - void at base	41	20	89**	37
P4	Grooved - end bearing	31	18	10**	110
P5A	Conventional - end bearing preload	30	23	29	130
P5B	Conventional - end bearing preload	30	28	42	70
P5C	Conventional - end bearing preload	30	30	48	110
P5D	Conventional - void at base	30	15	28	37

* Strain based on telltale measurements were determined using difference between middle and bottom telltale and only provide a crude approximation of strain in the test pier. (Accuracy of dial gauge = .001 in. is equivalent to a strain of 37×10^{-6})

** Readings may be erroneous due to difficulties with readout box.

The load distribution curves for conventional socketed piers, P1 and P2, at various magnitudes of applied load are shown in Figure 13. The distribution curves for test pier P1 (void at base) indicate that shaft resistance was distributed uniformly over the length of the socket for all values of applied load (Figure 13a). This distribution behavior is consistent with the load distribution predicted from analytical studies based on elastic theory (7). The distribution curves for pier P2 (load cell at base) are distinctly different from those of P1. In the elastic loading range $Q_T < 2.2$ MN, little shaft resistance was mobilized in the lower half of pier P2 (Figure 13b).

This behavior is not consistent with analytical solutions that predict uniform distribution of the load (constant slope) over the socket length (7). The reasons for this discrepancy are unclear. However, the similarity in the shape of the distribution curves for other similar piers suggests that the initial small preload applied to the base load cells (to ensure seating) may be the cause of this inconsistent behavior.

During the maintained load increment for pier P2 (applied load = 4.45 MN), the slopes of the upper and lower portions of the distribution curves began to equalize and load distribution or shaft resistance along the socket became essentially uniform at an applied load of 6 MN (Figure 13b).

CONCLUSIONS

The instrumentation used in a field testing program to investigate methods of improving the performance of rock socketed piers has been described and discussed. The results obtained from the test program demonstrate the reliability of the instruments used.

The load cells consisting of a series of FREYSSI flatjacks performed well. The load cells were reliable and the results obtained using these cells were estimated to be accurate to within ±2 percent.

In the case of test pier P1, the Geonor P-250 embedment vibrating wire strain gauges were judged to be reliable and satisfactory. All of the strain measurements for the test piers were consistent with anticipated behavior. When questionable data were obtained, the cause was improper grounding of the readout equipment and not a fault of the instruments themselves.

Loads (stresses) calculated using the strain gauge data enabled determination of the load distribution within the pier-socket system.

Displacement at the top, middepth, and bottom of the test piers and in the rock immediately adjacent to the piers was reliably measured using a combination of dial indicator gauges and telltale systems.

The versatility of a flatjack load cell to perform three different functions has been described.

ACKNOWLEDGMENTS

The work presented in this paper was performed by Western Caissons Limited. Financial support for the project was provided by Supply and Services, Canada, and the National Research Council (NRC) of Canada, under contract 1SX79.00053 and by the Natural Sciences and Engineering Research Council. The project was sponsored by the Division of Building Research, NRC. M. Bozozuk acted as scientific authority, made valuable suggestions for this work, and reviewed the

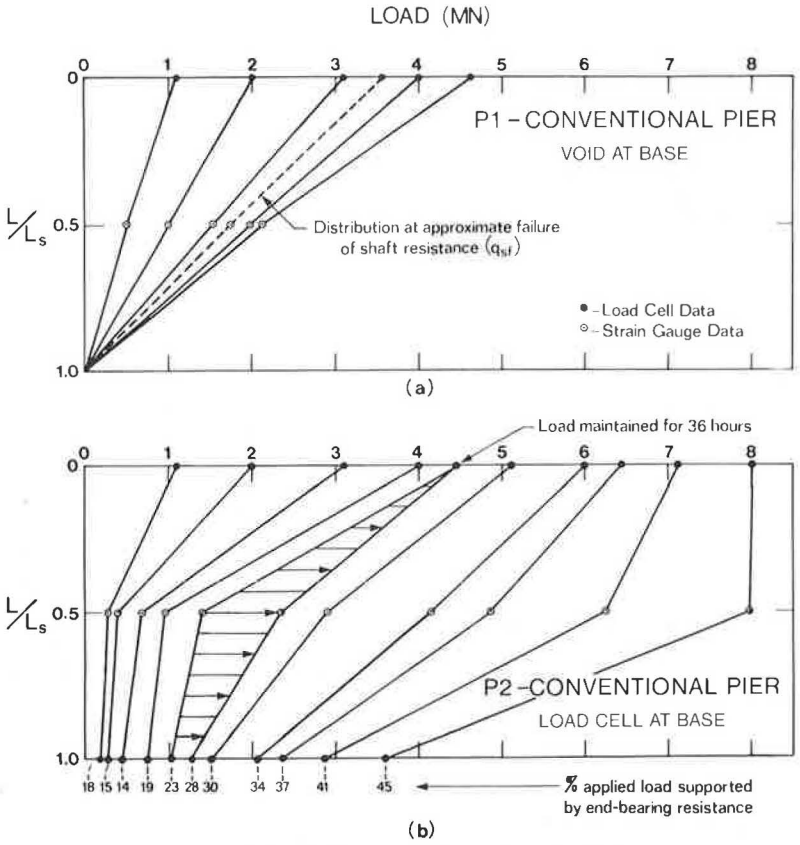

FIGURE 13 Typical load distribution curves for conventional piers.

manuscript. National Sewer Pipe provided use of the test site.

The author also acknowledges T.C. Kenney for his valuable assistance and D. Allan, J. Franklin, B. Fyfe, S. Horvath, P. Kozicki, P. Luk, E. Magni, R. Mills, B. Pluhator, and W. Trow for their contributions.

REFERENCES

1. R.G. Horvath. Drilled Piers Socketed into Weak Shale--Methods of Improving Performance. Ph.D. thesis. University of Toronto, Ontario, Canada, 1982.
2. R.G. Horvath, T.C. Kenney, and P. Kozicki. Influence of Shaft Roughness on Field Performance of Drilled Piers Socketed into Weak Shale. Proc., 34th Canadian Geotechnical Conference, Fredericton, New Brunswick, 1981, pp. 2.2.1 through 2.2.13.
3. M. Bozozuk, G.H. Keenan, and P.E. Pheeney. Analysis of Load Tests on Instrumented Steel Test Piles in Compressible Silty Soil. In Behavior of Deep Foundations, American Society for Testing and Materials Special Technical Publication 670, Raymond Lundgren, ed., 1979, pp. 153-180.
4. R.G. Horvath. Multiple Loading Method for Field Testing Drilled Piers. Submitted for publication to Canadian Geotechnical Journal, 1984.
5. P.J.N. Pells and R.M. Turner. Elastic Solutions for the Design and Analysis of Rock-Socketed Piles. Canadian Geotechnical Journal, Vol. 16, No. 3, Aug. 1979, pp. 481-487.
6. O.C. Zienkiewicz. The Finite Element Method in Engineering Science. McGraw-Hill, London, England, 1979, Ch. 5.
7. J.O. Osterberg and S.A. Gill. Load Transfer Mechanism for Piers Socketed in Hard Soils or Rock. Proc., 9th Canadian Rock Mechanics Symposium, Montreal, Quebec, 1973, pp. 235-262.

Closing Remarks on Reliability of Geotechnical Instrumentation

JOHN DUNNICLIFF

ABSTRACT

In the closing remarks delivered at the Symposium on Reliability of Geotechnical Instrumentation, three subjects are discussed: a "recipe" for reliability, the parameters that can be measured most readily, and a plea to users of instrumentation.

These closing remarks will address three topics: First, a recipe for reliability. Second, which parameters can be measured most reliably? Third, a plea to users of instrumentation.

A RECIPE FOR RELIABILITY

When this symposium was being planned, I wrote a recipe for reliability. Having now read the six papers that have been presented, I have made a few changes and will define what I believe are the major ingredients. There are two types: instrument ingredients (three of these) and people ingredients (five of these).

Instrument Ingredients

Simplicity

Follow the KISS (keep it simple, stupid) principle. For example, mechanical and hydraulic devices are generally more reliable than electrical devices.

Self-Verification

This term means that instrument readings can be verified in place. For example:

- Telltales on a rod extensometer with a method of disconnecting the rod from the anchor, so that a check can be made for free sliding;
- Duplicate transducers (e.g., a vibrating wire and a pneumatic transducer packaged within the same housing to create a piezometer with two independent methods of reading); and
- Checking remote-reading borehole extensometers with a dial gauge at the head.

Durability in the Installed Environment

The transducer must have proven longevity to suit the application. Cables, tubes, or pipes that connect the transducer to its readout must be able to survive imposed pressure changes, deformation,